ChemComm

COMMUNICATION

View Article Online
View Journal | View Issue

Cite this: *Chem. Commun.*, 2017, 53, 3022

Received 28th January 2017,
Accepted 17th February 2017

DOI: 10.1039/c7cc00769h

rsc.li/chemcomm

A neutral dinuclear Ir(III) complex for anti-counterfeiting and data encryption†

Yang Jiang,[a] Guangfu Li,[a] Weilong Che,[a] Yingjie Liu,[b] Bin Xu,[b] Guogang Shan,[a] Dongxia Zhu,*[a] Zhongmin Su*[a] and Martin R. Bryce*[c]

A neutral dinuclear Ir(III) Schiff base complex PIBIP has been synthesized and shown to exhibit both piezochromic luminescence (PCL) and aggregation induced emission (AIE) behaviour. An efficient second-level anti-counterfeit trademark and a data encryption device were fabricated using PIBIP as the active material.

Anti-counterfeiting and data security are important issues in the economy and military fields as well as in our everyday lives.[1] This has led to the development of technologies such as infrared up-conversion,[2] magnetic response[3] and plasmonic security labels.[4] However, these systems are presently facing various problems such as poor stability and high reaction temperature (the calcination temperatures usually reach 800 °C).[5] Therefore, there is an urgent requirement for new advanced materials with high thermal stability and facile preparation to combat counterfeiting and information leakage.

Phosphorescent transition-metal complexes, such as Ir(III) systems, have great potential in this area due to their high luminescence quantum yields, easy handling, structural versatility and high photostability.[6] However, traditional phosphorescent materials are usually used for first-level data encryption, with the disadvantage of security information being exposed immediately under ultraviolet (UV) light illumination. This means that encoded data are not secure and can be easily substituted by compounds with a similar emission colour. Therefore, the design of novel luminescent materials with more covert and reliable anti-counterfeit features is an appealing challenge. Piezochromic luminescent (PCL) compounds are a class of "smart" materials whose fluorescence properties change in response to external pressure or mechanical grinding.[7] It has been shown that this process can be reversed and the original emission colour can be restored by altering the molecular packing mode in the solid state in response to external stimuli, such as heating or recrystallization.[8] Taking advantage of this reversible property, PCL materials are widely used in sensors, memory chips, and security inks.[9]

However, PCL compounds generally require sophisticated synthesis (>10 steps) to introduce different components into one molecule.[10] Moreover, similar to most conventional dyes, these luminophores suffer from aggregation caused quenching (ACQ), which results in low phosphorescence quantum yields in the solid state.[11] All the aforementioned drawbacks significantly limit the real-world applications of PCL materials. In contrast, aggregation-induced emission (AIE), as coined by Tang *et al.* in 2001,[12] is a property of compounds which emit weakly when dispersed in dilute solution but show strong emission when aggregated due to restricted intramolecular motions. This abnormal phenomenon has attracted considerable interest in the field of electroluminescent devices and chemical sensing.[13] The motivation for the present work is to develop phosphorescent transition-metal complexes with combined AIE and PCL properties and to exploit them as candidates for applications in anti-counterfeiting and data encryption.

Herein, we designed and synthesized a new dinuclear Ir(III) complex $(ppy)_2$Ir-(bsbd)-Ir$(ppy)_2$ (**PIBIP**) with a Schiff base bridging ligand ($bsbdH_2$) and phenylpyridine (ppy) cyclometalating ligands (Scheme S1, ESI†). The photophysical properties demonstrate that **PIBIP** is AIE active and simultaneously shows PCL properties. Moreover, the emission colour of **PIBIP** can be converted to the original colour upon simple treatment by an organic solvent. These results lead to the demonstration of a second-level anti-counterfeit trademark and data encryption device using **PIBIP** as the security ink. **PIBIP** is the first neutral dinuclear Ir(III) complex which exhibits both PCL and AIE characteristics, to the best

[a] *Key Laboratory of Nanobiosensing and Nanobioanalysis at Universities of Jilin Province, Department of Chemistry, Northeast Normal University, 5268 Renmin Street, Changchun, Jilin Province 130024, P. R. China. E-mail: zhudx047@nenu.edu.cn, zmsu@nenu.edu.cn*
[b] *Key Laboratory of Supramolecular Structure and Materials, Institute of Theoretical Chemistry, Jilin University, Changchun 130012, P. R. China*
[c] *Department of Chemistry, Durham University, Durham, DH1 3LE, UK. E-mail: m.r.bryce@durham.ac.uk*

† Electronic supplementary information (ESI) available: Experimental details, ^{1}H NMR spectra, absorption and emission spectra, and crystallographic data. CCDC 1527325. For ESI and crystallographic data in CIF or other electronic format see DOI: 10.1039/c7cc00769h

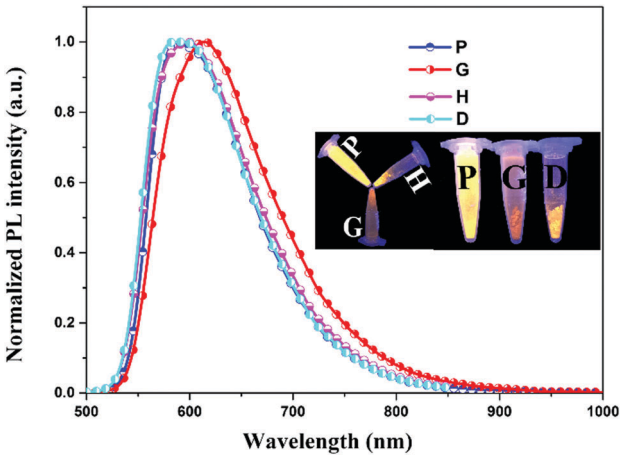

Fig. 1 Emission spectra of the unground "as synthesized" sample (**P**), ground sample (**G**), heated ground sample (**H**) and ground sample wetted with DCM (**D**). Inset: Emission image of **P**, **G**, **H** and **D** under 365 nm UV illumination.

of our knowledge. These combined properties are important for device applications.[7] The flexible nature of the bsbd spacer allows the ligand to adopt optimal coordination geometries at the metal centres so as to facilitate the coexistence of PCL and AIE.

The structure of **PIBIP** was established by its ^{1}H NMR and mass spectra, and single-crystal X-ray structure (ESI†). The pristine solid sample of **PIBIP** (hereafter abbreviated as **P**) shows yellow phosphorescence (λ_{max} = 587 nm), as shown in Fig. 1. When powder **P** was thoroughly ground in an agate mortar for 5 min, a significant bathochromic shift (λ_{max} = 613 nm) was observed in the orange-emitting ground sample **G** (Fig. 1). The emission intensity of **G** shows a significant weakening that is clearly visible to the naked eye. The photoluminescence quantum yield (PLQY) is decreased dramatically in the grinding process from 20% (**P**) to 7% (**G**) (Table S1, ESI†). To investigate the reversibility of this PCL behavior, **G** was wetted with dropwise addition of dichloromethane (DCM) solvent (sample **D**) and the emission colour reverted to the initial emission colour of **P** within a few seconds (Fig. 1). Notably, the emission could perfectly revert to **G** when **D** was further ground. This PCL behaviour of **PIBIP** was shown to be highly reversible for several grinding–wetting cycles (Fig. S4, ESI†).

In order to establish the origin and mechanism of this reversible piezochromic behaviour of **PIBIP**, the ^{1}H NMR spectra of both **P** and **G** were obtained. The results show complete consistency of chemical shift values and peak shapes for both **P** and **G** (Fig. S1, ESI†). The changed phosphorescent colours in the grinding process are, therefore, attributed to physical processes.

Powder X-ray diffraction (PXRD) was carried out to investigate the aggregation states of **P** and **G**. The sharp peaks in the XRD pattern (Fig. 2a) unambiguously indicate that the **P** sample has a well-ordered crystalline structure. In sharp contrast, the ground sample **G** exhibits weak and broad diffraction signals, which imply a crystalline to amorphous phase transition during the grinding process. The clear reflection peaks of pristine solid **P** reappeared after sample **G** was heated (sample **H**) or wetted

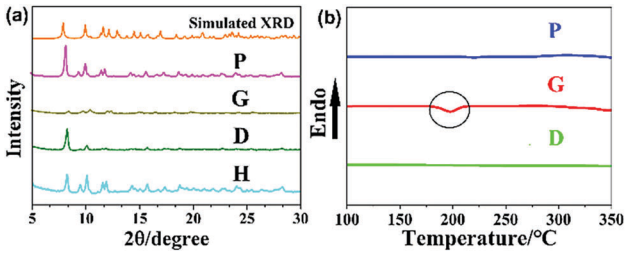

Fig. 2 Powder X-ray diffraction patterns (a) and the DSC traces (b) of the corresponding samples.

with DCM solvent dropwise (sample **D**). In addition, upon heating **G** to 350 °C, the DSC traces exhibited a clear broad exothermic recrystallization peak at *ca.* 198 °C. This peak is at a similar temperature at which thermal recrystallization begins to take place (Fig. 2b). Therefore, when **G** was heated at 198 °C for 1 min, the crystalline state was recovered and consequently the emission colour reverted to the original one (Fig. 1). **PIBIP** emitted only weakly in amorphous **G**, but became strongly emissive in crystalline **P**. This is typical crystallization-induced emission enhancement (CIEE) behaviour.[14] These results provide a rational explanation for the variation in PL intensity.

The single crystal X-ray structure analysis of **PIBIP** demonstrates that no intermolecular interactions exist in the molecular packing (Fig. S8, ESI†). By contrast, obvious intramolecular π–π interactions between the bridging phenyl ring and the adjacent phenyl rings of ppy are observed (Fig. 3). This structure might be easily modified when mechanical pressure is applied, resulting in a red-shift of the PL spectra.[15] The excited-state lifetimes (τ) for **PIBIP** significantly decreased from **P** (0.97 μs) to **G** (0.49 μs) (Table S1, ESI†). Thus, it can be concluded that the changed τ in the PCL process is associated with alteration in the solid-state molecular packing and/or the intramolecular interactions. The similar τ values of both the **P** and **D** states are consistent with them having the same molecular arrangement.[16]

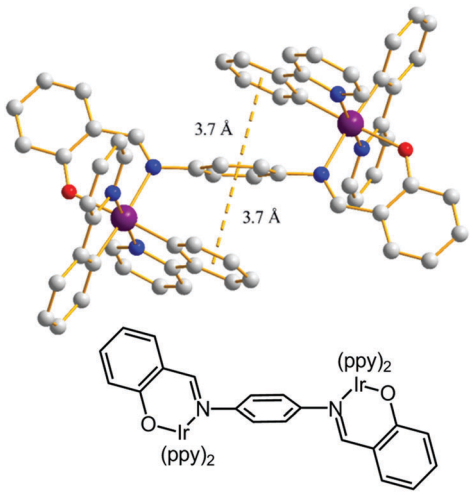

Fig. 3 The X-ray molecular structure of **PIBIP** showing intramolecular π–π interactions (dashed line). Colour code: Ir purple; N blue; O red.

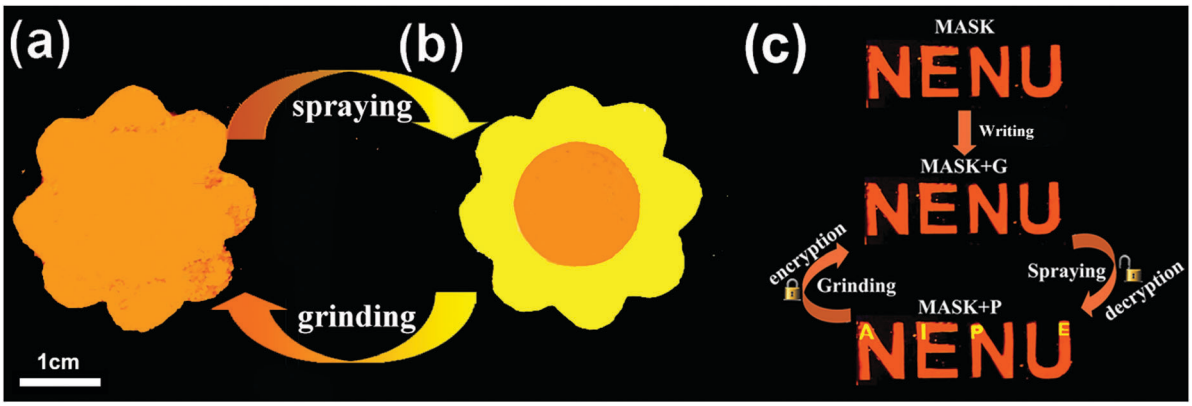

Fig. 4 Photographic images of the (a) first-level anti-counterfeit trademark, (b) second-level anti-counterfeit trademark and (c) information encryption and decryption devices. Note the appearance of the yellow letters 'AIPE' within the bottom 'NENU'.

Encouraged by the excellent PCL performance of **PIBIP**, anti-counterfeit trademark and data encryption devices were constructed (Fig. 4). **MASK** is a fluorescent emitter selected from the literature[17] (for the structure see Fig. S2 in the ESI†), which shows a similar emission peak to **G** at around 610 nm (Fig. S3, ESI†). Thus, it is difficult to distinguish **G** from **MASK** due to their very similar emission colours and emission intensities. Furthermore, no colour change is observed when mechanical grinding is applied to **MASK**, which is an exclusive method to differentiate **G** and **MASK** (Fig. S3, ESI†). As shown in Fig. 4a and b, the anti-counterfeit trademark adopted the shape of a 'flower' comprising a central 'stamen' and a 'petal'. The 'stamen' is the as-prepared powder of **MASK**, which emits orange fluorescence upon excitation with a 365 nm UV lamp and the 'petal' is the sample of **G** (the detailed method is given in the ESI†). This device could provide a second-level anti-counterfeit function. As shown in Fig. 4a, orange light was rapidly observed under the illumination of a standard UV lamp (at 254 and 365 nm), presenting a first-level anti-counterfeit system. When this 'flower' was sprayed with dichloromethane (DCM) solvent, the emission of the 'petal' changed immediately from orange (**G**) to yellow (**D**) (Fig. 4b). A second-level anti-counterfeit system was then successfully obtained as follows. Upon further grinding the 'petal', the original emission colour was regenerated and the first-level anti-counterfeit trademark reappeared (Fig. S5, ESI†).

Furthermore, a simple, convenient and efficient technology for data encryption and decryption was designed (Fig. 4c). **G** was used as a 'cryptographic ink', while **MASK** was used as a control reagent. In the encryption stage, the characters 'NENU' were written on a filter paper by using **MASK**, and then powder **G** was carefully spread on it as the letters 'AIPE'. So **G** was hidden by **MASK** even under UV light, because **G** and **MASK** emitted unitary orange light. In the decryption stage, the yellow security letters 'AIPE' appeared clearly when DCM solvent was sprayed onto the as-prepared letters 'NENU'. In contrast to the orange-emitting background, the letters 'AIPE' showed intense yellow emission, which is in agreement with the change in the emission colour from **G** to **D**. Moreover, 'AIPE' can be easily hidden again by grinding. This simple process demonstrates excellent encryption and decryption reversibility for several cycles. These data suggest that complex **PIBIP** has the potential to be employed in practical applications as an anti-counterfeit and security protection ink with simple optical authentication.

Since **PIBIP** exhibits strong luminescence in the solid state (Table S2, ESI†), the AIE property was probed by using different ratios of THF–water mixtures. As shown in Fig. 5, **PIBIP** exhibits very weak emission in pure THF solution, where it was well dissolved. Nevertheless, the PL intensity was dramatically enhanced when the water fraction reached 50%, increasing by a maximum of up to about 100-fold in comparison with the pure THF solution. The PL intensity then decreased with increasing water content $>50\%$ water fraction, but the PL intensity at 90% water fraction is still stronger than in the pure THF solution. There are two possible reasons for this behaviour. First, after aggregation, the molecules covered within the surface of the nanoparticles did not emit light, leading to a decrease in phosphorescence intensity. Second, crystalline particles and

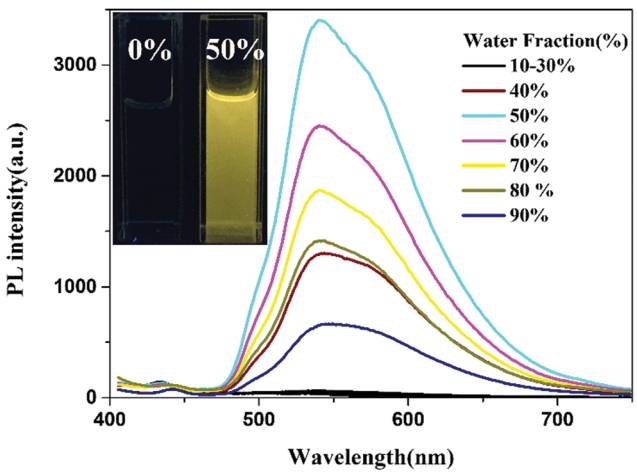

Fig. 5 Emission spectra of **PIBIP** in THF–water mixtures with different water fractions (0–90% v/v) at room temperature. Inset: Emission image of **PIBIP** in pure THF solution and the THF–water mixture (50% water fraction) under 365 nm UV illumination.

amorphous particles simultaneously form when the water fraction is increased. The former particles would enhance the emission intensity but the latter do not.[8] Thus, the measured overall PL intensity depends on the combined actions of the two kinds of nanoparticles. Furthermore, the UV-visible absorption profile showed a Mie scattering effect for the mixtures of **PIBIP** with high water content (Fig. S6, ESI†).[18] Transmission electron microscopy (TEM) and electron diffraction (ED) experiments indicated that amorphous molecular aggregates are formed in the mixtures (Fig. S7, ESI†).[19] Evidently, **PIBIP** is an excellent AIE chromophore that could effectively suppress non-radiative decay to produce intense emission in the solid state.

In summary, a smart dinuclear Ir(III) Schiff base complex **PIBIP** shows simultaneous reversible PCL behaviour and AIE-activity. An obvious bathochromic shift occurs in the solid state upon mechanical grinding, and this new emission reverts to the original state after wetting with DCM solvent. Anti-counterfeiting trademark and data encryption devices have been successfully constructed by combining **PIBIP** and fluorescent **MASK** through the piezochromic and solvatochromic properties of **PIBIP**. Therefore, these findings indicate that **PIBIP** could expand the applications of PCL materials to anti-counterfeiting, information storage and data security protection.

The work was funded by the NSFC (No. 51473028), the Key Scientific and Technological Project of Jilin Province (20150204011GX, 20160307016GX), and the Development and Reform Commission of Jilin Province (20160058). Work in Durham was funded by EPSRC grant EP/K039423/1.

Notes and references

1 (*a*) M. You, M. Lin, S. Wang, X. Wang, G. Zhang, Y. Hong, Y. Dong, G. Jin and F. Xu, *Nanoscale*, 2016, **8**, 10096–10104; (*b*) M. You, J. Zhong, Y. Hong, Z. Duan, M. Lin and F. Xu, *Nanoscale*, 2015, **7**, 4423–4431; (*c*) T. Zhang, L. Fu, Z. Chen, Y. Cui and X. Liu, *Prog. Org. Coat.*, 2016, **100**, 100–104; (*d*) P. Kumar, S. Singh and B. K. Gupta, *Nanoscale*, 2016, **8**, 14297–14340.

2 J. F. Suyver, A. Aebischer, D. Biner, P. Gerner, J. Grimm, S. Heer, K. W. Krämer, C. Reinhard and H. U. Güdel, *Opt. Mater.*, 2005, **27**, 1111–1130.

3 R. Li, Y. Zhang, J. Tan, J. Wan, J. Guo and C. Wang, *ACS Appl. Mater. Interfaces*, 2016, **8**, 9384–9394.

4 Y. Cui, R. S. Hegde, I. Y. Phang, H. K. Lee and X. Y. Ling, *Nanoscale*, 2014, **6**, 282–288.

5 J. M. Meruga, W. M. Cross, P. Stanley May, Q. Luu, G. A. Crawford and J. J. Kellar, *Nanotechnology*, 2012, **23**, 395201.

6 (*a*) H. Sun, S. Liu, W. Lin, K. Y. Zhang, W. Lv, X. Huang, F. Huo, H. Yang, G. Jenkins, Q. Zhao and W. Huang, *Nat. Commun.*, 2014, **5**, 3601; (*b*) H. Sasabe, J. Takamatsu, T. Motoyama, S. Watanabe, G. Wagenblast, N. Langer, O. Molt, E. Fuchs, C. Lennartz and J. Kido, *Adv. Mater.*, 2010, **22**, 5003–5007; (*c*) M. Mydlak, C. Bizzarri, D. Hartmann, W. Sarfert, G. Schmid and L. De Cola, *Adv. Funct. Mater.*, 2010, **20**, 1812–1820.

7 Z. Chi, X. Zhang, B. Xu, X. Zhou, C. Ma, Y. Zhang, S. Liu and J. Xu, *Chem. Soc. Rev.*, 2012, **41**, 3878–3896.

8 (*a*) M. Luo, X. Zhou, Z. Chi, S. Liu, Y. Zhang and J. Xu, *Dyes Pigm.*, 2014, **101**, 74–84; (*b*) Q. Lu, X. Li, J. Li, Z. Yang, B. Xu, Z. Chi, J. Xu and Y. Zhang, *J. Mater. Chem. C*, 2015, **3**, 1225–1234; (*c*) X. Zhang, Z. Ma, Y. Yang, X. Zhang, Z. Chi, S. Liu, J. Xu, X. Jia and Y. Wei, *Tetrahedron*, 2014, **70**, 924–929.

9 (*a*) A. Pucci, F. Di Cuia, F. Signori and G. Ruggeri, *J. Mater. Chem.*, 2007, **17**, 783–790; (*b*) Y. Dong, J. W. Y. Lam, A. Qin, J. Liu, Z. Li, B. Z. Tang, J. Sun and H. S. Kwok, *Appl. Phys. Lett.*, 2007, **91**, 011111; (*c*) Z. Ning, Z. Chen, Q. Zhang, Y. Yan, S. Qian, Y. Cao and H. Tian, *Adv. Funct. Mater.*, 2007, **17**, 3799–3807; (*d*) S. Hirata and T. Watanabe, *Adv. Mater.*, 2006, **18**, 2725–2729; (*e*) A. Kishimura, T. Yamashita, K. Yamaguchi and T. Aida, *Nat. Mater.*, 2005, **4**, 546–549.

10 C. Ma, B. Xu, G. Xie, J. He, X. Zhou, B. Peng, L. Jiang, B. Xu, W. Tian, Z. Chi, S. Liu, Y. Zhang and J. Xu, *Chem. Commun.*, 2014, **50**, 7374–7377.

11 Z. Zhang, Z. Wu, J. Sun, P. Xue and R. Lu, *RSC Adv.*, 2016, **6**, 43755–43766.

12 J. Luo, Z. Xie, J. W. Y. Lam, L. Cheng, B. Z. Tang, H. Chen, C. Qiu, H. S. Kwok, X. Zhan, Y. Liu and D. Zhu, *Chem. Commun.*, 2001, 1740–1741.

13 J. Mei, N. L. Leung, R. T. Kwok, J. W. Lam and B. Z. Tang, *Chem. Rev.*, 2015, **115**, 11718–11940.

14 J. Tong, Y. J. Wang, Z. Wang, J. Z. Sun and B. Z. Tang, *J. Phys. Chem. C*, 2015, **119**, 21875–21881.

15 (*a*) Y. Dong, B. Xu, Y. J. Zhang, X. Tian, L. Wang, J. Chen, H. Lv, S. Wen, B. Li, L. Ye, B. Zou and W. Tian, *Angew. Chem., Int. Ed.*, 2012, **51**, 10782–10785; (*b*) Q. Qi, J. Qian, X. Tan, L. Wang, B. Xu, B. Zou and W. Tian, *Adv. Funct. Mater.*, 2015, **25**, 4005–4010.

16 Y. Han, H. T. Cao, H. Z. Sun, Y. Wu, G. G. Shan, Z. M. Su, X. G. Hou and Y. Liao, *J. Mater. Chem. C*, 2014, **2**, 7648–7655.

17 R. K. Shah, K. S. Abou-Melha, F. A. Saad, T. Yousef, G. A. A. Al-Hazmi, M. G. Elghalban, A. M. Khedr and N. El-Metwaly, *J. Therm. Anal. Calorim.*, 2015, **123**, 731–743.

18 B. Xu, W. Li, J. He, S. Wu, Q. Zhu, Z. Yang, Y.-C. Wu, Y. Zhang, C. Jin, P.-Y. Lu, Z. Chi, S. Liu, J. Xu and M. R. Bryce, *Chem. Sci.*, 2016, **7**, 5307–5312.

19 G. G. Shan, H. B. Li, J. S. Qin, D. X. Zhu, Y. Liao and Z. M. Su, *Dalton Trans.*, 2012, **41**, 9590–9593.